Comparative Study on Various Microbolometer Structures

Article · December 2015

CITATIONS
0

READS
30

5 authors, including:

Cezary Maj
Lodz University of Technology
42 PUBLICATIONS **50** CITATIONS
SEE PROFILE

Wojciech Zabierowski
Lodz University of Technology
114 PUBLICATIONS **66** CITATIONS
SEE PROFILE

A. Napieralski
Lodz University of Technology
399 PUBLICATIONS **879** CITATIONS
SEE PROFILE

Comparative Study on Various Microbolometer Structures

Jacek Nazdrowicz, Michał Szermer, *Member*, *IEEE*, Cezary Maj, Wojciech Zabierowski, and Andrzej Napieralski, *Senior Member*, *IEEE*

***Abstract*—Meaningful progress in the fields of MEMS is associated with the continuous development of the micromachining technologies. One of the most promising devices in MEMS is thermal sensors. When the first microbolometer appeared on the market, a huge interest in thermal detectors was observed. This paper is a short overview study on microbolometer geometry, different solutions and possibilities to implement them as electrical models.**

***Index Terms*—microbolometer, MEMS, microsystems, thermal imaging, integrated circuits.**

I. Introduction

IN recent years, the intensive development in MEMS area is observed. It is caused by constantly increase demand on smart devices with various functionalities. The meaningful technology transfer from science to industry plays here also an important role. One of the most dynamically developed areas is infrared radiation (IR) detection, which is applied in many contemporary devices. The most known MEMS IR detector is a microbolometer.

Devices used for IR detection were well-known, before the era of miniaturization. After Herschel discovered in XIX century this type of radiation, some scientists: Kirchhoff, Stefan, Boltzmann, Planck and Wien gave mathematical and physical foundation for building thermal detectors. Discovering infrared energy beyond the visible region and commonly used part of electromagnetic spectrum aroused great interest of many scientists. In 1878 an American astronomer Langley invented a bolometer. It was designed to measure solar radiation energy, but it was quickly adapted to other applications [1]-[3]. Its main benefit was a capability to detect the infrared radiation objects from hundreds of meters away and is sensitive to differences in temperature of one hundred-thousandth of a degree Celsius. This bolometer consisted of Wheatstone's bridge and galvanometer.

Nowadays, micromachining technology allows designing and fabrication of the complex systems for thermal imaging, which are lighter, smaller, easier and more comfortable in use than in those times [4],[5].

J. Nazdrowicz, M. Szermer, C. Maj, W. Zabierowski and A. Napieralski are with the Department of Microelectronics and Computer Science, Lodz University of Technology, ul. Wólczańska 221/223, 90-924 Lodz, Poland (e-mail: jnazdrowicz@dmcs.pl).

II. Microbolometer Structure and Operation

A typical microbolometer consists of some characteristic parts: a membrane thermally isolated from its surroundings by legs, anchors and a substrate (Fig. 1a). The membrane (Fig. 1b) is the main part, which absorbs radiation. It consists of a heat-sensitive layer, covered by two protective films. Thermal isolation of the membrane is ensured by combining it with thin legs connected to the silicon substrate via anchors. The legs have two functions: protect the membrane from destruction due to its deformation during the heating and connect the sensor to the readout integrated circuit (ROIC). Moreover, the legs dimensions allow minimizing the conductivity impact on a temperature measurement, because the membrane is thermally isolated from environment. As can be seen in Fig. 1b, thermal isolation of an active film detector from its surroundings is achieved thanks to the usage of the two thin legs. Heat conduction is most critical when neighbour detectors are very close and heat transfer can occur between them. The less important is heat convection, which can be practically eliminated by encapsulation of the detector in vacuum.

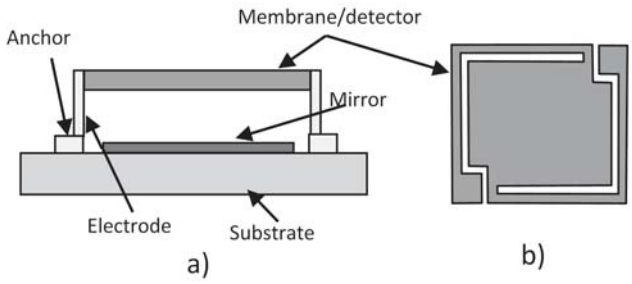

Fig. 1. Structure of the microbolometer: a) cross section [9], b) top view.

An additional element of the microbolometer is a mirror placed under the membrane. The main task of it is to reflect the falling heat, which improve the performance of the sensor. When we look at the cross-section of the microbolometer, it can be seen that this is a very complex object. It consists of several layers. In order to achieve required mechanical, thermal and electrical parameters, different materials should be used. It has to be noticed that one of the main limitation is the dimension of the microbolometer. In microscale only a dedicated micromachining technology can be used.

ISSN 2080-8755

The principle of operation of the microbolometer is based on a resistance measurement. A bias current applied to the structure between the membrane legs causes the current flow through the detecting conductor placed within the membrane. IR sensitivity conductor changed its resistance as a result of the falling radiation that heats up the structure. This causes the voltage change in the structure.

The principle of operation of the microbolometer is presented in Fig. 2. Incident radiation, which falls on the detecting layer generate the temperature increase $\Delta T=E/C$. This occurs until radiation energy in absorber is equal to energy in heat sink, flowing through the legs, which have small thermal conductance G. Absorber, which has the specific heat capacity C and absorption η, cumulates the heat energy, which directly affects the absorber electrical resistance and causes the changes in the current flow. This absorber simply acts as a thermistor. As it can be seen, the most important in the microbolometer is the heat flow between particular elements. The simple thermal model of the microbolometer that consists of the detector, substrate and environment parameters was presented in [6].

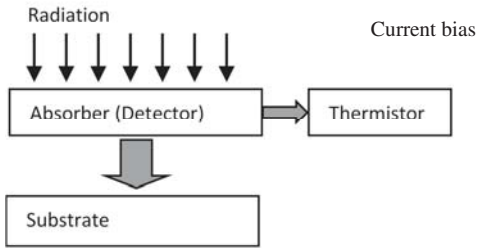

Fig. 2. Microbolometer principle operation.

A fundamental equation for IR detectors is a heat flow equation. The differential heat equation of the microbolometer including the self-heating effect is as follows [7]:

$$C\frac{d(\Delta T)}{dt}+G(\Delta T)=P_{IR}+P_{BIAS} \tag{1}$$

where P_{IR} is the IR power absorbed by the microbolometer detector, P_{BIAS} is the bias power connected with joule heating, C is the thermal capacitance and G is the thermal conductance of microbolometer.

When microbolometer detectors are exposed to incident IR, change in incoming radiant flux can be expressed by the following formula,

$$\Delta\phi_{IR}=\frac{A_b\Delta T_s}{4F^2}\left(\frac{dP}{dT}\right) \tag{2}$$

where A_b is the area of microbolometer detector, ΔT_s is the difference in target and ambient temperature, F is the *f*/number of the optical system and (dP/dT) is change in power per unit area with respect to temperature change radiated by black body at an ambient temperature in the wavelength interval of 8μm-14μm. Incoming radiant flux changes the temperature of thermal detectors and change in temperature due to the absorbed infrared power can be calculated as:

$$\Delta T_{IR}=\frac{\Delta\phi_{IR}}{G} \tag{3}$$

We distinguish generally two modes of microbolometer operation. The first one based on the constant bias current that flows through the structure and the second one based on the pulse bias current. Both solutions have advantages and disadvantages. The most important advantage of the second solution is the power dissipation reduction in the sensor in comparison of the first one mode of operation.

The microbolometer step response vs. current bias where it operates in the pulse mode is shown in Fig. 3. We distinguish three phases in the microbolometer work: rise phase, steady phase and fall phase. During the rise phase, temperature of the microbolometer increases. After that phase it is stabilized on the constant level. When we turn off the current bias, temperature of the microbolometer decreases. Time of these phases depends on the duty cycle of the current bias pulse.

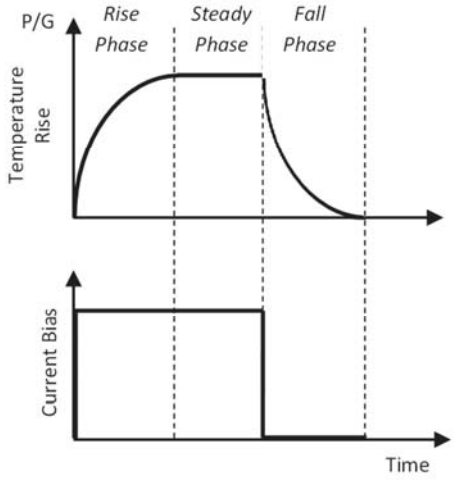

Fig. 3. Microbolometer pulse response.

All the thermo-sensing materials must have a large temperature coefficient of resistance (*TCR)*. Large *TCR* means that a small change of the detector temperature causes a large resistance change. Thus, it has an influence on the microbolometer's performance: responsivity (ability to convert falling radiation into an electrical signal), *1/f* noise (which causes the disturbances of a signal) and resistance (impacts a power consumption of detector's operation).

There are many materials used in microbolometer fabrication - Titanium (*Ti*), Vanadium Oxide (*VO*), Yttrium Barium Copper Oxide (*YBaCuO*, *YBCO*), *GeSiO*, poly *SiGe*, *BiLaSrMnO*, Amorphous Silicon *α-Si*, *poly-Si*. The last two are commonly applied in thermal detectors. Although semiconductor's microbolometers are more sensitive, *Ti*-based detectors with high bias current have better responsivity without degrading their sensitivity [9].

Recent research on microbolometers leads to assemble them in vacuum, which eliminates the air thermal convection loss.

III. GEOMETRY

Nowadays, the geometry of the microbolometers is diverse. There are some key elements, which may differ from each other: membrane, supporting legs, absorbing conductor shape, reflecting mirror location. During designing process there are many factors, which should be taken into consideration to ensure that the device will be appropriate for the future application.

Since the microbolometer basic geometry has been used, it is constantly improved in order to achieve a better performance. There are some key features taken into account:

- electrical parameters,
- mechanical properties of applied materials,
- power consumption,
- size of detector.

When you look at the detector from the top side, two characteristic elements, membrane and supporting legs can be seen.

Supporting legs play a very important role. Appropriate design of these elements influence on reduction of the heat loss, flowing from the membrane to the substrate. Agreeing with the thermal conductance equation, the thermal conductance of supporting legs can be expressed as [10]:

$$G_{leg} = \kappa_{leg} \frac{w_{leg} h_{leg}}{l_{leg}} = \sum_i \kappa_i \frac{w_i h_i}{l_i} \tag{4}$$

where: κ_{leg} is the thermal conductivity, w_{leg}, l_{leg}, h_{leg}, are supporting legs' dimensions: width, length and height respectively. The quantities with i index are referred to particular layers of supporting legs.

The thermal conductance is inversely proportional to the length. Simultaneously, length of the legs is determined by a distance between the membrane and the substrate [10]. This is why, in many geometries legs are long and bent (Fig. 4a).

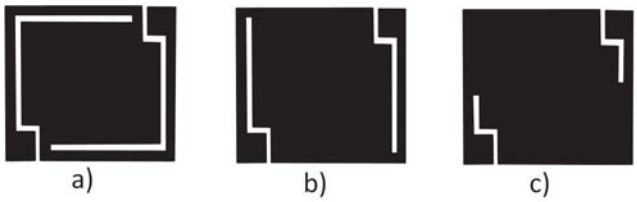

Fig. 4. Various geometries membrane and supporting legs.

The membrane with short supporting legs is presented in Fig. 4c. This detector's geometry can be successfully applied to the microbolometers constructed with amorphous silicon (α-Si). Additionally, having the possibility to design very thin legs and membrane of microbolometer based on α-Si, the thermal insulation of it is much higher than in VO_x based one. Thus, using such geometry the pixel's dimension is smaller. As a result the pixels' density per unit area is higher. Consequently, this is a good solution for increasing the resolution of microbolometer array. In the year 2000, the pixel pitch was achieved on 45 μm level giving 320×240 resolution array; now 17 μm is achieved, what gives the possibility to design and fabrication arrays with 1024×768 resolution [11]. Simplified geometry impacts the number of operations in fabrication process and cost reduction, thus they are widely commercialized.

The optimization of supporting legs found in literature (called meshed structure) is associated with improvement performance and structural stability of microbolometers [12]. It is very good in order to achieve the high-resolution array (Fig. 5). Additional advantage of this is simple control of time constant by increasing or decreasing the number of holes.

Generally, there are two approaches of anchors design in the microbolometer array. First, the most popular solution is the individual anchors for each supporting leg in the microbolometer membrane. Second, there are common anchors for neighbour structures (two or four).

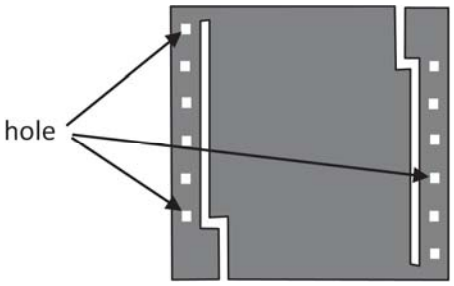

Fig. 5. Meshed structure of microbolometer supporting legs.

In order to improve the detector performance a reflecting mirror is applied as it was mentioned earlier. There are two main approaches: mirror is placed on the substrate or above it as a bottom layer of the membrane. In both cases mirror is located under detecting layer, because the membrane is partially transparent for incident radiation. This solution decreases the measurement inaccuracy of the incident radiation. It is described in details in [13]-[14]. In Fig. 6 the differences between these approaches are presented. Fig. 6a presents a traditional configuration, where the distance between the membrane and the mirror is about a quarter of a radiation wavelength. Fig. 6b presents the structure, where optical cavity is formed within the membrane. As a result, the total thickness of the membrane is larger and must be fit for optimal absorption, i.e. with manipulating refractive index.

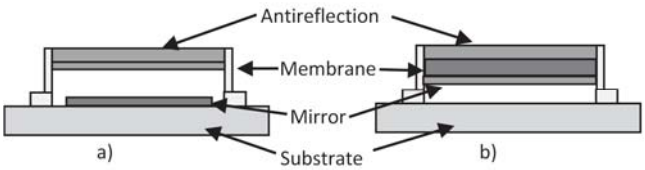

Fig. 6. Mirror location in microbolometer: a) on substrate, b) on membrane [16]

The most important part of the microbolometer is a detector conduction layer. It is often placed between two outer protective layers, which are built with various materials. In publications many different absorber shapes can be found. The

different geometry is tested in the following publications [17], [18]. The most popular geometry is serpentine of various shapes (Fig. 7). More complex serpentines include additionally uniform beams and extrusions for absorbers. Some of them have a large area of absorber. This geometry will be analysed in our simulations.

IV. Modelling and Simulations

In order to find optimal shape of the microbolometer a lot of simulations should be performed. It is important in the face of huge costs of the prototype manufacturing. Simulations help to avoid these problems by analysing the model of the microbolometer.

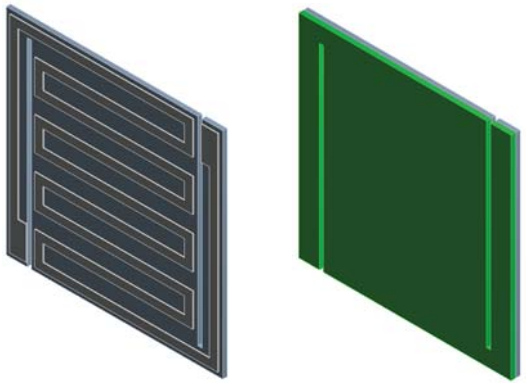

a) b)

Fig. 7. Microbolometer structure view: a) active layer, b) active and insulating layers.

The analysis of the microbolometer is quite complex. There are many phenomena, which should be taken into account. Therefore, multidomain simulations have to be performed.

Generally, two methods are used: the analysis using finite element method (FEM) and the analysis using equivalent electric circuit model. The FEM model is more complex and time consuming while the equivalent circuit model is easier in implementation and faster in calculation. However, FEM model is more accurate and allows including all phenomena while the equivalent circuit model is more limited and has some simplifications.

In many publications the circuit model allows simulating a joule heating effect and/or noise sources. One of the circuit model often described in publications is presented in Fig. 8. This model does not contain the noise sources. However, current or voltage sources that represent various types of noise are often implemented.

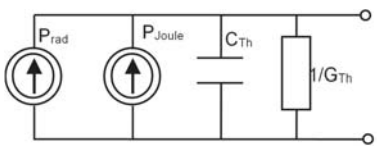

Fig. 8. Circuit model of microbolometer with Joule-heating effect [19].

In the FEM model is necessary to mesh the structure. It allows discretizing the model and solves the differential equations in characteristic points called nodes with the assumption of proper boundary conditions and loads. The FEM model is often applied to simulate a heat distribution in protective membrane layers as well as in absorbent. Authors often apply such model for comparing it with circuit models to verify results and conclude if simpler circuit model is designed correctly [19].

The equivalent circuit model is very useful if the ROIC is used in analysis. The ROIC is necessary to read and process signals from the sensor. Usually, this is an electronic circuit, which consists of Wheatstone bridge and amplifier. In such circuit there are two microbolometers. One is a reference structure and the second is a measuring structure. In this way, it is possible to observe the difference in output signals in both structures. This is a differential method of measurement.

Nowadays, there are many implementations of ROIC in microbolometers' applications. Scientists are constantly improving these devices in order to reduce the number of noise sources or at least to minimize their influence on a measurement process.

In literature various circuit models can be found. These models have different level of details. However, all of them implement a mutual dependence between thermal and electrical domains (Fig. 9).

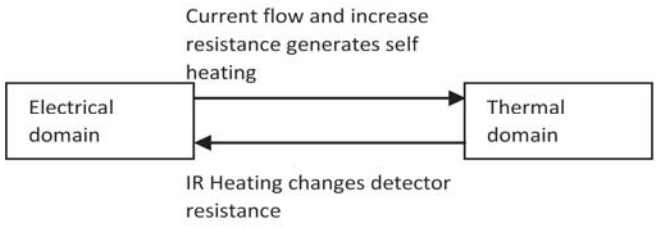

Fig. 9. Mutual dependency between electrical and thermal domains in microbolometers.

More accurate description of coupling between electrical and thermal domains is presented in [19]. This model takes into account the heat radiation and the current flow through the sensor depending on the temperature.

In the circuit model all phenomena should be implemented. They should be described by equivalent electrical equations. The following electrical elements are used: resistors, capacitors, and voltage and/or current sources (independent and controlled). Then, it is possible to describe the following phenomena:

- infrared radiation,
- heat,
- current flow,
- noise.

The equations that describe the thermal domain must be transformed into equivalent equation in electrical domain (Table I [20]).

TABLE I
ANALOG THERMAL AND ELECTRICAL QUANTITIES

Symbol	Thermal Quantity	Symbol	Electrical Quantity
ΔT	Temperature difference	V	Voltage
P	Absorbing power	I	Current
R	Thermal resistance	R	Electrical resistance
C	Thermal capacitance	C	Electrical capacitance
G	Thermal conductance	G	Electrical conductance

A. Simple circuit model

The simplest dynamic circuit model of microbolometer (Fig. 10a), found in literature [21] consists of resistor (detector) and current source (bias), where $\Phi(t)$ is the radiation flux, $I_{bias}(t)$ is the bias current, $V_{out}(t)$ is the output voltage [22]. However, the model shown in Fig. 5a does not reflect the effect of a thermal capacity. This effect could be represented by an additional capacitor C (Fig. 10b).

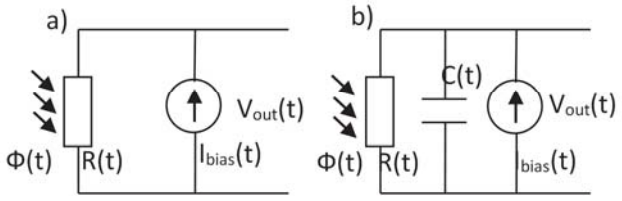

Fig. 10. Microbolometer simple circuit models: a) without heat capacitance [20], b) with heat capacitance [23].

Resistance of the detector can be found by calculating total absorbing conductor resistance with TCR agreeing to well-known formula:

$$R = \rho \frac{d}{A} \tag{5}$$

where ρ is the resistivity, A is the section area, d is the length of conductor.

The effective thermal resistance is a complex quantity. The detecting layer is placed between two protective layers. Thus the total thermal resistance is equal to the resistance of parallel connection of two legs [24]:

$$R_{TH} = \frac{1}{G_{TH}} = \frac{1}{2G_{leg}} \tag{6}$$

where G_{leg} is given by the equation 4. Consequently, we have to calculate the effective thermal resistance of a block composed of two materials. It can be shown that in such a case, the effective thermal resistance can be calculated as a parallel connection of the thermal resistances of both materials [24]. The thermal capacity of the bolometer can be calculated using the formula [9]:

$$C_{TH} = \sum_{i}^{n} v_i \rho_i c_i \tag{7}$$

where v_1, v_2, … ρ_1, ρ_2 …, c_1, c_2,… are the volumes, densities, mass specific heats, respectively of the bolometer membrane material layers. The thermal capacity expresses detecting area of the microbolometer. This is a thermal mass, which absorbs heat energy [25]. If the volume of active layer is significantly smaller than this of insulating membranes, it can be neglected. This model is very popular in literature [26]-[29]. In this form it can be very useful for simulations, because it reflects very important problem that determine model usability, which is related to a dynamic parameter such as thermal time-constant. This problem is met in infrared cameras and limits theirs frame rate.

Moreover, it is desired to put an additional element, which expresses the heat loss through the radiation. This is done by adding a thermal conductance G_{rad}. It has significant impact especially when the thermal conductance G_{leg} is comparable to the radiation conductance G_{rad}. Thermal conductance can be expressed by multiplying the derivative of the total exitance of a body and the bolometer area $2A_d$ (because both, the top surface and the bottom surface of the microbolometer are radiating) [30]:

$$G_{rad} = 2A_d \frac{d\eta\sigma T^4}{dT} \tag{8}$$

where σ is the Stefan-Boltzmann constant and η is the absorptivity of the body.

B. Bias current and Joule effect

As it was mentioned earlier, the principle of operation of the microbolometer is based on a resistance change. This requires DC bias current to be applied to the device. It allows reading the change in resistance due to absorbed radiation by a detection film. The high responsivity is achieved by applying large current. Unfortunately, the current flow through the resistive layer leads to the heating of the structure (Joule heating effect). This has a negative impact on the structure [31]. Hence, it must be corrected by the factor P_{JH} (dissipated Joule heat) [32] appearing on the right side of the equation 1:

$$C\frac{d(\Delta T)}{dt} + G(\Delta T) = P_{IR} + P_{BIAS} + P_{JH} \tag{9}$$

In order to reduce Joule heat emission the bias current in the microbolometer should be a pulse. Joule heat potentially produces a thermal energy, which impacts on the device performance (noise equivalent temperature difference NETD). It is important to highlight the optimum performance of the detector. The temperature distribution and response of the detector in different thermal conditions and loads should be considered during the design phase. Additionally, if the pulse width increases, the NETD is reduced. However, characterizing the thermal behaviour for different loads of a given microbolometer it is very important to understand its performance and reliability. The thermal characteristic of the device itself also changes the physical properties of the multi-layered structure, which in turn, affects the performance and lifetime of the microbolometer [33].

One of the simplest models with Joule heating effect presented in literature contains two sources and RC elements (Fig. 11) [19]. It was developed for analysing the device during initial design process. Joule heating in this model was

simulated using current source P_{Joule}. Radiation was also implemented as a current source P_{rad}. This approach is commonly used in many circuits models, e.g. in measurement the thermal behaviour of a microbolometer array [34].

More complex model is presented in [35]. Authors stated that to do proper bias current optimization, the model needs to incorporate electrothermal effects and one cannot reflect all phenomena with only resistor-based microbolometer. Bias heating effect is very important consideration in microbolometers, because increasing bias current allows obtaining better responsivity. Proposed model shows that responsivity depends on *TCR*, thermal conductance *G* and time constant τ, and it should not neglect impact of these parameters. This model (see Fig. 12) takes into consideration Joule effects, resistivity of contacts R_s and other parasitic resistances R_p. Current that cause Joule heating is described as a controlled current source $I=P_E$. Radiation power is presented as another controlled current source $I=\eta P_{IR}$. To reflect initial temperature value, there is an additional current source I_{BK} placed in parallel. In result, the temperature rise (represented by voltage) increases the electrical resistance that cause a recursive feedback process.

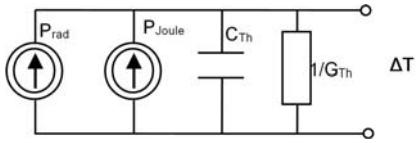

Fig. 11. Circuit model of microbolometer with Joule-heating effect [19].

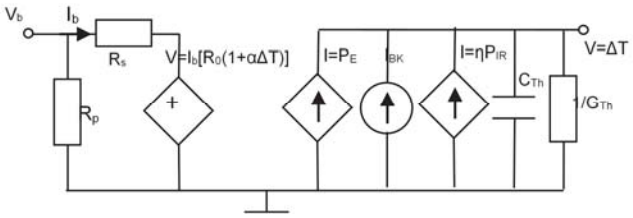

Fig. 12. Microbolometer model proposed in [35].

This model was implemented in Simulink package (without R_s and R_p), Fig. 13. Voltage source is replaced with direct connection of model output signal with input user-defined function block *Fcn* to implement dependency.

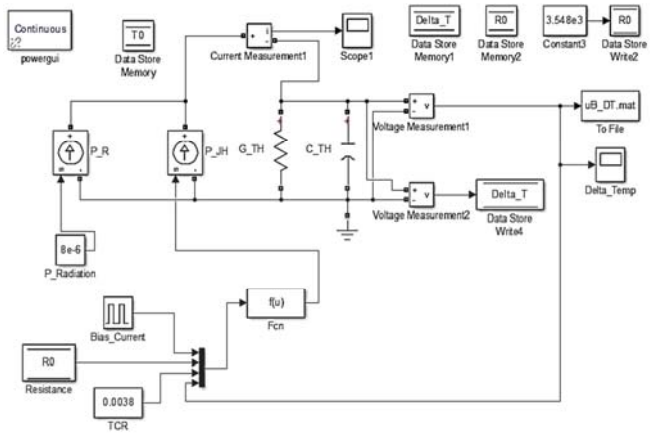

Fig. 13. Implementation complex circuit model of microbolometer in SIMULINK.

C. Geometry calculations

Circuit model of microbolometer does not allow implementing exact geometry such as shape of a microbolometer, shape of supporting legs or shape of a detecting layer. To do this, it is necessary to use FEM model. In the circuit model it can be applied necessary geometry parameters such as: length, height, width of the active layer. In our calculations we use the parameters listed in the Table II (value of each parameter is shown in Table III further in the text). The geometrical variables are explained in Fig. 14.

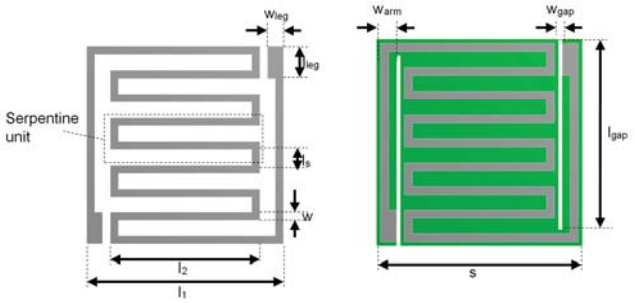

Fig. 14. Microbolometer dimensions: a) serpentine active layer, b) insulating layer.

TABLE II
LIST OF GEOMETRICAL AND MATERIAL PARAMETERS.

Symbol	Quantity
l_1	Active layer size
l_2	Active layer inner size
w	Active layer width
h	Active layer height
l_{leg}	Leg length
w_{leg}	Leg width
h_{leg}	Leg height
s	Membrane size
h_t	Top membrane height
h_b	Bottom membrane height
l_{gap}	Gap length
w_{gap}	Gap width
w_{arm}	Arm width
r	Electrical resistivity of active material
κ_a	Thermal conductivity of active material
α	Temperature coefficient of resistance of active material
κ_i	Thermal conductivity of insulating material
ρ	Density of insulating material
c	Specific heat of insulating material
n	Serpentine count
l_s	Short length of serpentine

Note that for simulation reason, serpentine count is separately denoted as *n*. The serpentine unit consists of 4 parts: 2 long conductors and 2 short conductors. The length can be calculated using the following formula:

$$l_{serp} = 2(l_2 - w) + 2(l_s - w) \tag{10}$$

Total length of the active layer conductor is:

$$l_{total} = nl_{serp} + 2\left[\left(l_1 - l_{leg}\right) - w\right] + \left[\left(l_1 - l_2\right) - 2w\right] + l_2 \tag{11}$$

Of course, the condition which must be fulfilled is as follows:

$$n(2l_s - w) < l_1 \tag{12}$$

This condition guarantees that total width of serpentine will be less than width of the active layer).

D. Simulations

In our simulations we analysed self-heating effect of the structure. This effect has negative impact on measurement reliability because it causes an additional temperature increase inside the structure. This depends directly on the geometrical dimensions of the active layer.

Some simulations were performed with Simulink model presented in Fig. 13. Table III presents the list of parameters and theirs values used in simulations [36]. We investigated the influence of some parameters on the behaviour of the structure. These simulations show the impact of geometrical dimensions on self-heating resulting in temperature rise.

Fig. 15 shows characteristic of microbolometer temperature rise in case of various serpentine counts. It can be seen that maximal temperature rise in the first cycle is smaller about 15-20 % than next ones, what confirms establishing temperature in active layer of the microbolometer. In next cycles the peak stabilizes. The offset of linear characteristic presented in Fig. 16 equal to 2.61 comes from the fact, that even though serpentine count is 0, temperature rise exists, due to existence of supporting legs resistance.

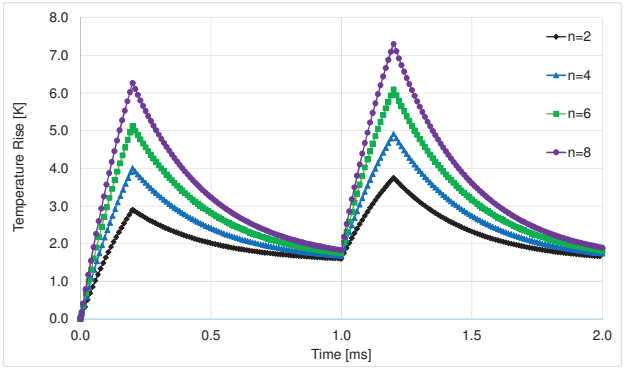

Fig. 15. Temperature rise for various serpentine counts.

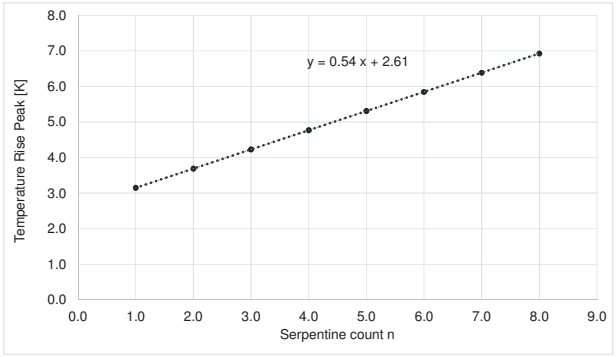

Fig. 16. Linear dependency between temperature rise and serpentine count.

In the following simulation the width of detecting layer varied in the range of 0.4-1.0 µm. The results are presented in Fig. 17. We can see that temperature rises significantly with decrease of the active layer width. The temperature peak needs a few cycles to stabilize.

Thanks to power approximation and use of appropriate equation one can estimate expected temperature rise for a given detecting layer width. Nonlinear characteristic causes that there is a limit that temperature rise will stabilize. This is an optimal value of the detecting layer width (Fig. 18). We have to take into consideration that parameters of this equation are not constant and depend mainly on other geometrical dimensions and parameters.

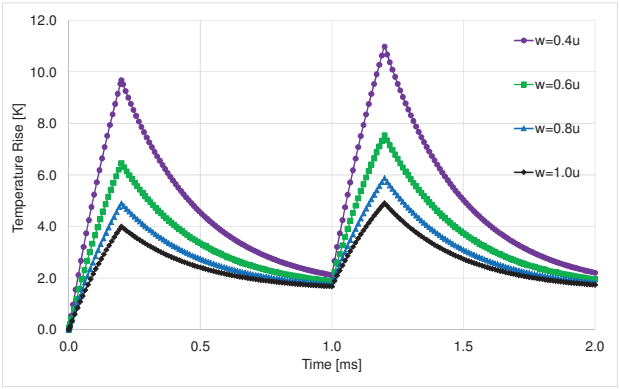

Fig. 17. Temperature rise of microbolometer for various width of detecting layer in time.

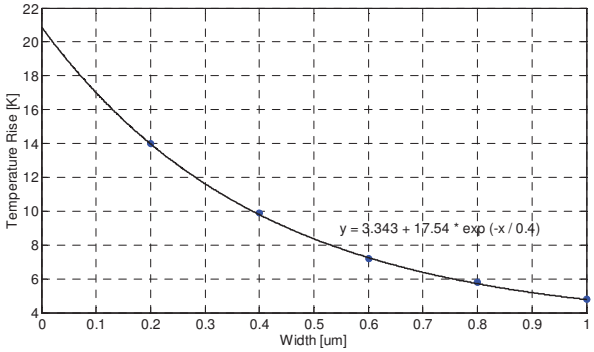

Fig. 18. Temperature rise for microbolometer for various width of detecting layer and its approximation.

Optimization of the microbolometer geometry needs to be done together with current bias source parameters. As it can be seen in Fig. 19, the temperature of microbolometer strongly depends on bias current. Above I_b=100 µA the temperature rise resulting from the self-heating effect grows significantly (dependence is in square) what influences negatively on the measurement process. That is why the good idea is to decrease this influence by changing microbolometer dimensions. Decreasing the current from I_b=200 µA to 75 µA the temperature rise drops from 8.6 K to 1.4 K. (see Fig. 19).

In previous simulations the value of the current was modified. In a further simulation pulse period is analysed. The results are presented in Fig. 20. The increase of pulse period has an influence on the increase of the temperature rise peak value. In each case the time constant in the rise phase is the same as it depends only on model RC parameters. However,

the rise time is of course different in each case. In our case, the rise phase is short and does not allow reaching steady state value. In the fall phase it can be observed that there is the same minimal value of temperature for all cases as this phase is long enough to reach steady state. Of course, increase of the pulse period has the negative impact on detection usability, because time between two radiation measurements becomes longer.

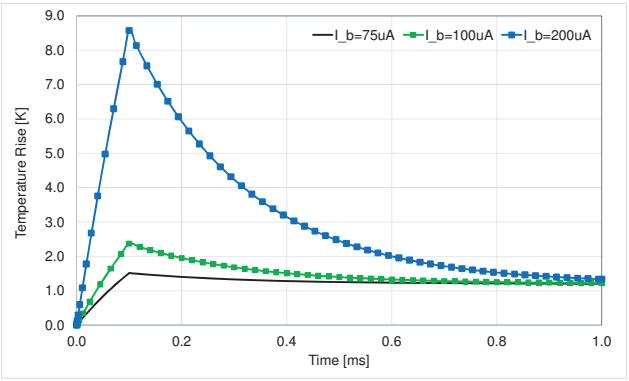

Fig. 19. Dependency between temperature rise and time with various current value of bias source.

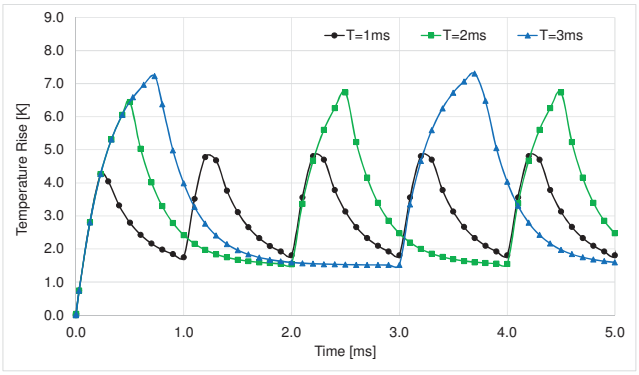

Fig. 20. Temperature rise for various bias pulse period.

Another parameter taken into account in simulations was the duty cycle of the current pulse. For given geometric parameter set (Table III) it influences on temperature rise during each cycle (Fig. 21). The behaviour is similar to previous simulations (for entire cycle time) but detection intervals are the same. In these simulations period time was T=1 ms. Along with pulse time increase, temperature rises. Moreover, similar to Fig. 18 maximal temperature value is reached slower.

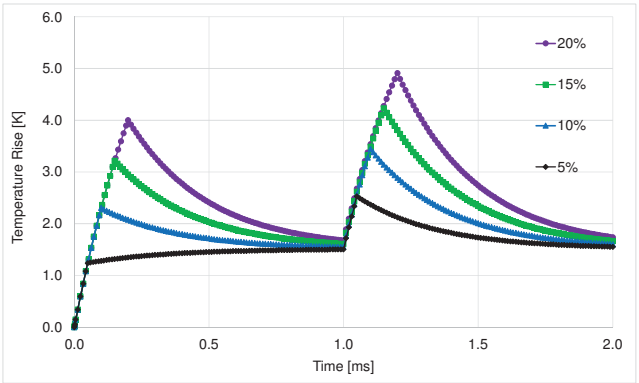

Fig. 21. Temperature rise for various bias pulse duration.

TABLE III
PARAMETERS SET USED IN SIMULATIONS

Quantity	Value	Quantity	Value
l_1 [μm]	25	w_{gap} [μm]	0.5
l_2 [μm]	19	w_{arm} [μm]	2.5
w [μm]	1	r [Ωm]	1.6E-6
h [μm]	0.1	κ_a [$Wm^{-1}K^{-1}$]	22
l_{leg} [μm]	4	α[1/K]	3.8E-3
w_{leg} [μm]	2	κ_i [$Wm^{-1}K^{-1}$]	30
h_{leg} [μm]	2	ρ [kg/m^3]	3290
s [μm]	26	c [$Jkg^{-1}K^{-1}$]	700
h_t [μm]	0.5	R_{TH}[K/W]	1.89E-5
h_b [μm]	0.5	C_{TH}[J/K]	1.56E-9
l_{gap} [μm]	24	R[Ω]	3.51E3

V. Current and Future Works

Relying on actual achievements in MEMS area, principle of operation, designing and performance aspects with modern fabrication technologies, future works will be concentrated on some very important aspect of microbolometers:

- creating models appropriate for simulation,
- optimization of membrane geometry and legs structure based on simulation results,
- detect noise levels in circuit model and compensate them with electronic circuit,
- optimize power need for sensor operation based on bias current,
- improve principal detector parameters like detectivity, responsivity, time constant and resolution.

Looking at the above simulations, it will be able to help in improvement of microbolometer performance especially taking into account:

- decrease influence of Joule effect - lower impact on resistivity of microbolometer and its usefulness,
- material selection - under physical properties and potential use in microbolometers,
- thermal isolation and decrease heat loss between membrane and substrate layer,
- microbolometer geometry - shape and dimensions, location of ROIC in microbolometer pixel array, vacuum in sensor package for minimizing heat energy convection to other detectors,
- optimize time constant - time resolution of detector;
- decrease influence of noises - noise level produced during operation and signal processing in CMOS integrated circuits technology.

As it can be seen above, there are many areas of microbolometers that can be developed. New techniques and technologies still open areas for new research.

VI. Conclusions

Thermal sensors have wide application in many areas of our life. Presented current state of microbolometers detectors as well as fabrication methods and future works shows that this is very complicated structure, especially in designing and construction devices with larger resolution and wide range of temperature without additional cooling systems.

Intensive development of MEMS devices causes thermal detector development, discovering various materials application thus obtaining various microbolometers structures, parameters and performance. This allows applying them in many systems where high quality and miniaturization is required.

In order to design the microbolometer properly many simulations should be performed. We have here two approaches. We can use a FEM model or electrical circuit model of the microbolometer. In this paper we present the electrical circuit model of microbolometer. This model does not allow us to implement exact geometry of particular microbolometer part, it is possible to simulate it providing accurate results calculating electrical parameters of the detecting layer. The most important parts of the detector can be successfully modelled using physical quantities and laws. In case of active layer it can be done with parallel or series connection of resistances. In case of more sophisticated shapes of active layer to calculate resistance it would be necessary to use complex calculations.

The authors of the paper presented microbolometers circuit microbolometer model created in MATLAB/Simulink, which was verified in previous work [36]. Simulations results are promising and give foundations for further microbolometer optimization such as geometry, material properties and bias parameters. This will be in further research expanded and compared with the FEM model.

ACKNOWLEDGEMENTS

The results presented in this paper were supported by Marie Curie International Research Staff Exchange Scheme Fellowship within the 7th European Community Framework Programme, Project: Developing Multidomain MEMS Models for Educational Purposes - EduMEMS, no. 269295.

REFERENCES

[1] H. Kaplan, “Practical Applications of Infrared Thermal Sensing and Imaging Equipment”, SPIE Optical Engineering Press, 1993.

[2] R. J. Dempsey, D.G. Davis, R.G. Jr. Bruice and R.A. Lodder. “Biological and Medical Applications of Near Infrared Spectrometry” in *Applied Spectroscopy*, Vol.50 (2), pp. 18A-34A, 1996.

[3] P.W. Kruse, “Uncooled Thermal Imaging Arrays, Systems, and Applications”, SPIE Press, 2001.

[4] E. L. Dereniak, G. D. Boreman. „Infrared Detectors and Systems”, John Wiley and Sons, 1996, s. 395- 438.

[5] P.R. Norton, “Infrared Detectors in the Next Millennium”, Proc. SPIE, Vol. 3698, pp. 652–665. 1999.

[6] X. Chen, K. Wu, “A new bias equalization for microbolometer array”, Symposium on Photonics and Optoelectronics, Chengdu, China, pp. 1-4, June 19-21, 2010.

[7] S.I. Haider, S. Majzoub, M. Alturaigi, M. Abdel-Rahman, “Column-Wise ROIC Design for Uncooled Microbolometer Array”, in *Proc. International Conference ICTRC*, Abu Dhabi, United Arab Emirates, pp. 56-59, May 17-19, 2015.

[8] P.W. Kruse, D.D. Skatrud, “Uncooled infrared imaging arrays and systems”, Semiconductors and Semimetals, Vol. 47, Academic Press, London 1997.

[9] R. S. Saxena, R. K. Bhan, C. R. Jalwania, and Kumkum Khurana, “Effect of Excessive Bias Heating on a Titanium Microbolometer Infrared Detector”, IEEE Sensors Journal, Vol. 8, No. 11, pp. 1801-1804, November 2008.

[10] K. Sandeep, D. Butler, “Infrared Sensing With Self-Supporting YBCO Uncooled IR Microbolometer Array Integrated With On-Chip CCBDI Readout Circuit”, IEEE Sensors Journal, Vol. 9, No. 4, p. 414, April 2009.

[11] http://www.sofradir-ec.com/wp-uncooled-detectors-achieve.asp (22/06/2016).

[12] K. Young Su, K. Tae Hyun, K. Gyung Tae, L. Boo Taek, L. Seong Kyu, L. Hi Deok, and L. Ga Won, “Uncooled Microbolometer Arrays With High Responsivity Using Meshed Leg Structure”, IEEE Photonics Technology Letters, Vol. 25, No. 21, pp. 2108-2110, November 1, 2013.

[13] F. Niklaus, C. Vieider, H. Jakobsen, “MEMS-Based Uncooled Infrared Bolometer Arrays” in *A Review, MEMS/MOEMS Technologies and Applications III*, edited by C. Jung-Chih, C. Xuyuan, Y. Zhaoying, L. Xinxin, Proc. of SPIE, Vol. 6836, 68360D, 2007.

[14] S-B. Ju, Y-J. Yong, S-G. Kim, “Design and fabrication of a high fill-factor micr-bolometer using double sacrificial layers”, SPIE, Vol. 3698, Infrared Technology and Applications, XXV, 1999.

[15] R.A. Wood, “Uncooled Microbolometer Infrared Sensor Arrays” in [Infrared Detectors and Emitters: Materials and Devices] ed. Capper P. and Elliott, C.T., Kluwer Academic Publishers, Norwell, 2001.

[16] F. Niklaus, et al., “Performance model for uncooled infrared bolometer arrays and performance predictions of bolometers operating at atmospheric pressure”, Infrared Physics & Technology 51(3), pp. 168-177, 2008.

[17] W. Chang, Y. Liang, “Geometric Design of Microbolometers Made From CMOS Polycrystalline Silicon”, IEEE Sensors Journal, Vol. 15, No. 1, p. 265, January 2015.

[18] X. He, G. Karunasiri, T. Mei, W. J. Zeng, P. Neuzil, and U. Sridhar, “Performance of Microbolometer Focal Plane Arrays Under Varying Pressure”, IEEE Electron Device Letters, Vol. 21, No. 5, p. 234, May 2000.

[19] P. Zając, C. Maj, M. Szermer, M. Lobur, A. Napieralski, “Analytical tool for electro-thermal modelling of microbolometers”, in Proc. International Conference on Thermal, Mechanical and Multi-Physics Simulation and Experiments in Microelectronics and Microsystems, EuroSimE, Gent, Belgium, pp. 1-6, April 7-9, 2014.

[20] N. H. Sabah, “Electric circuits and signals”, CRC Press, Boca Raton, p. 784, 2007.

[21] D. Wurfel and H. Vogt, “An improved electrical and thermal model of a microbolometer for electronic circuit simulation”, Adv. Radio Sci., 10, pp. 183–186, 2012.

[22] H. M. Oloomi, M. S. Alam, and M. M. Rana, “Noise Performance Evaluation of Uncooled Infrared Detectors” (June 2009), IEEE Sensors Journal, Vol. 11, No. 4, pp. 971-972, April 2011.

[23] P. Zając, C. Maj , M. Szermer, M. Lobur, A. Napieralski, “Analytical Thermo-electric Model of Uncooled Microbolometer”, Machine Dynamics Research, Vol. 37, No 3, p.102, 2013.

[24] E. Iborra, M. Clement, L. Herrero, “Sangrador IR uncooled bolometers based on amorphous GeSiO on silicon micromachined structures”, Journal of Microelectromechanical Systems, Vol. 11, No. 4, pp. 322-329, 2002.

[25] H. Lee, J. Yoon, E. Yoon, S. Ju, Y. Yong, W. Lee, S. Kim, “A high fill-factor infrared bolometer using micromachined multilevel electrothermal structures,” IEEE Transactions on Electron Devices, Vol. 46, pp. 1489-1491, July 1999.

[26] F. Utermöhlen, I. Herrmann, “Model and Measurement Technique for Temperature Dependent Electrothermal, Parameters of Microbolometer Structures”, DTIP Barcelona, Spain, 16-18 April 2013.

[27] H. Budzier, G. Gerlach, “Thermal Infrared Sensors, in Thermal Infrared Sensors: Theory, Optimisation and Practice”, John Wiley & Sons, Ltd, Chichester, UK, 2011.

[28] V. Szekeley, „A new evaluation method of thermal transient measurement results“, Microelectronics Journal, Vol. 28, No. 3, pp. 277-292, 1997.

[29] M. Marz, P. Nance, “Thermal Modeling of Power-electronic Systems”, Technical report, Fraunhofer Institute for integrated circuits IIS-B, Erlangen, 2000.

[30] J. Nazdrowicz, M. Szermer, C. Maj, W. Zabierowski and A. Napieralski, “A Study on Microbolometer Electro-thermal Circuit Modelling”, in *Proc. International Conference MIXDES*, Torun, Poland, pp. 458-463, June 25-27, 2015.

[31] G. Li, N. Yuan, J. Li, X. Chenc, "Thermal Simulation of Micromachined Bridge and Self-heating", Journal of Sensors and Actuators A, 126, pp. 430–435, 2006.

[32] P. Neuzil, T. Mei, "A Method of Suppressing Self-Heating Signal of Bolometers", IEEE Sensors Journal, Vol. 4, No. 2, p. 208, April 2004.

[33] M. Almasri, Z. Celik-Butler, D. Butler, A. Yaradanakul, A. Yildiz, "Semiconducting YBaCuO microbolometers for uncooled broad-band IR sensing", Proc. of the SPIE, Vol. 4369, pp. 264-273, 2001.

[34] G. Bieszczad, M. Kastek, "Measurement of thermal behavior of detector array surface with the use of microscopic thermal camera", Metrology and Measurement Systems, Vol. XVIII, No. 4, pp. 679-690, 2011.

[35] R. S. Saxena, A. Panwar, S. S. Lamba, R.K. Bhan, "A sub-circuit model of a microbolometer IR detector and its experimental validation", Sensors and Actuators A 171, pp. 138-145, 2011.

[36] J. Nazdrowicz, "A study on microbolometer electro-thermal circuit modelling", in *Proc. International Conference MIXDES*, Torun, Poland, pp. 458-463, June 25-27, 2015.

Jacek Nazdrowicz was born in Poddębice, Poland, in 1975. He received the MSc degrees in Technical Physics, Computer Sciences and Marketing and Management from the Lodz University of Technology, Poland, in 1999, 2000 and 2001 respectively and the PhD degree in Economics Sciences, Management discipline, in Lodz University of Technology, in 2013.
From 2014 he attends doctoral study in Lodz University of Technology, electronics discipline. His research interests include modelling and simulation MEMS devices and their application in medicine. He also participates in EduMEMS project (Developing Multidomain MEMS Models for Educational Purposes).
Since 2007 he also works in mBank as a System Engineer of SQL Server databases. He has the following certifications: MCSA Windows 2012, MS SQL Server 2012 and Storage Area Network (SAN) Specialist.

Michał Szermer was born in Łódź, Poland, in 1973. He received the MSc and PhD degrees from Lodz University of Technology, Poland, in 1998 and 2004, respectively. His research focuses on the integrated circuits design with special consideration of mixed-signal circuits. He took part in many projects connected with ASICs design. Recently, he is involved in MEMS modelling and design as a coordinator of the EduMEMS project in the frame of 7th FP of EU who focused on development of new MEMS structures for educational purposes.

Cezary Maj was born in Łódź, Poland, in 1982. He received the MSc degree in electronics from Lodz University of Technology (TUL), Poland, in 2005 and PhD degree in microelectronics from both TUL and Institut National des Sciences Appliquées de Toulouse, France. He specializes in microelectronics and his research focuses on modelling, fabrication and characterization of microsystems. He took part in a few project connected with development of sensors for various applications. Recently, he is involved in MEMS modelling and investigation of thermal problems in current multicore processors.

Wojciech Zabierowski (Assistant Professor at Department of Microelectronic and Computer Science Technical University of Lodz) was born in Lodz, Poland, on April 9, 1975. He received the MSc and PhD degrees from the Technical University of Lodz in 1999 and 2008, respectively. He is an author or co-author of more than 100 publications: journals and most of them - papers in international conference proceedings. He has been reviewer in dozens international conferences. He supervised more than 100 MSc theses. He is focused on internet technologies, MEMS technologies and automatic generation of music. He is working in linguistic analysis of musical structure.

Andrzej Napieralski received the MSc and PhD degrees from the Technical University of Lodz (TUL), Poland in 1973 and 1977, respectively, and a DSc degree in Electronics from the Warsaw University of Technology, Poland and in Microelectronics from the Universite´ de Paul Sabatie´r, France in 1989. Since 1996 he has been Director of the Department of Microelectronics and Computer Science. Between 2002 and 2008 he was Vice-President of TUL. He is an author or co-author of over 960 publications and editor of 19 conference proceedings and 12 scientific Journals. He has supervised 45 PhD theses; six of them received the Prime Minister of Poland prize. In 2008 he received the Degree of Honorary Doctor of Yaroslaw the Wise Novgorod State University, Russia.